Multiple functions of LIM domain-binding CLIM/NLI/Ldb cofactors during zebrafish development

ELSEVIER

Mechanisms of Development 117 (2002) 75–85

www.elsevier.com/locate/modo

Multiple functions of LIM domain-binding CLIM/NLI/Ldb cofactors during zebrafish development

Thomas Becker, Heather P. Ostendorff, Michael Bossenz, Anne Schlüter, Catherina G. Becker, Reto I. Peirano, Ingolf Bach*

Zentrum für Molekulare Neurobiologie Hamburg (ZMNH), Universität Hamburg, Martinistrasse 85, 20251 Hamburg, Germany

Received 13 September 2001; received in revised form 10 May 2002; accepted 13 May 2002

Abstract

The crucial involvement of CLIM/NLI/Ldb cofactors for the exertion of the biological activity of LIM homeodomain transcription factors (LIM-HD) has been demonstrated. In this paper we show that CLIM cofactors are widely expressed during zebrafish development with high protein levels in specific neuronal cell types where LIM-HD proteins of the Isl class are synthesized. The overexpression of a dominant-negative CLIM molecule (DN-CLIM) that contains the LIM interaction domain (LID) during early developmental stages of zebrafish embryos results in an impairment of eye and midbrain–hindbrain boundary (MHB) development and disturbances in the formation of the anterior midline. On a cellular level we show that the outgrowth of peripheral but not central axons from Rohon Beard (RB) and trigeminal sensory neurons is inhibited by DN-CLIM overexpression. We demonstrate a further critical role of CLIM cofactors for axonal outgrowth of motor neurons. Additionally, DN-CLIM overexpression causes an increase of Isl-protein expression levels in specific neuronal cell types, likely due to a protection of the DN-CLIM/LIM-HD complex from proteasomal degradation. Our results demonstrate multiple roles of the CLIM cofactor family for the development of entire organs, axonal outgrowth of specific neurons and protein expression levels.

Keywords: LIM homeodomain factor; CLIM/NLI/Ldb cofactor; Eye; Midbrain–hindbrain boundary; Axonal projection; Zebrafish

1. Introduction

LIM homeodomain (LIM-HD) transcription factors have been demonstrated to be responsible for the regulation of many cellular processes during the development of organisms as divergent as *Drosophila* and higher vertebrates (Bach, 2000; Hobert and Westphal, 2000; Dawid and Chitnis, 2001). Besides their requirement for the development of specific neuronal cell populations such as motor- and interneurons (Pfaff et al., 1996; Jurata et al., 2000), LIM-HD proteins are essential for the formation of many other neuronal and non-neuronal structures (Bach, 2000; Hobert and Westphal, 2000). Recently, LIM homeodomain genes have also been shown to be involved in the regulation of axonal pathfinding (Sharma et al., 1998; Thor et al., 1999; Kania et al., 2000; Segawa et al., 2001). The identification of the LIM domain as a protein-protein interaction domain resulted in the isolation of several LIM domain-interacting cofactors (Bach, 2000; Dawid and Chitnis, 2001), including the homodimer-forming CLIM cofactor family that consists of CLIM1/Ldb2 and CLIM2/NLI/Ldb1/Chip (Agulnick et al., 1996; Jurata et al., 1996, 1998; Bach et al., 1997; Morcillo et al., 1997) and the RING zinc finger protein RLIM (Bach et al., 1999). Subsequently, it has been shown that the binding of cofactors to the LIM domain results in a variety of different consequences for the activity conferred by LIM-HD proteins (Bach, 2000; Dawid and Chitnis, 2001). Depending on the examined promoter, the association of CLIM cofactors to LIM domains of LIM-HD proteins is either important for gene activation events (Bach et al., 1997; Mochizuki et al., 2000) or results in an inhibition of gene expression (Jurata and Gill, 1997). Indeed, a requirement of dimerizing CLIM cofactors for at least some of the in vivo activities of LIM-HD proteins has been demonstrated (Agulnick et al., 1996; Jurata and Gill, 1997; Morcillo et al., 1997; Bach et al., 1999; Milán and Cohen, 1999; van Meyel et al., 1999, 2000). In addition, it has been shown that the cellular CLIM protein concentrations are critical determinants of LIM-HD activity in vivo (Rincon-Limas et al., 2000).

* Corresponding author. Tel.: +49-40-42803-5668; fax: +49-40-42803-8023.

E-mail address: ingolf.bach@zmnh.uni-hamburg.de (I. Bach).

0925-4773/02/$ - see front matter
PII: S0925-4773(02)00178-8

In this paper we have investigated the in vivo function of CLIM cofactors by ectopically overexpressing a dominant-negative CLIM molecule (DN-CLIM) early during zebrafish development, thereby impairing the interactions between cofactors and LIM proteins. We show that this overexpression results in the inhibition of eye and midbrain–hindbrain boundary (MHB) development, perturbation of axonal outgrowth of specific neuronal cell types, and changes in gene expression. Since disturbances of specific LIM-HD genes have been shown to result in similar effects (Bach, 2000; Hobert and Westphal, 2000), we conclude that protein interactions mediated by LIM domains are important for at least some of the biological functions which are conferred by the LIM-HD transcription factor family during vertebrate development.

2. Results

2.1. CLIM cofactors are coexpressed with LIM-HD proteins in developing neurons

The in vivo activity of LIM-HD proteins is critically regulated by CLIM cofactors in a concentration-dependent fashion. To examine the role of CLIM cofactors for zebrafish development it was important to assess the CLIM cofactor tissue distribution at the protein level, since protein concentrations of this class of cofactors are tightly controlled (Ostendorff et al., 2002). We first tested our CLIM antiserum in Western blots on adult zebrafish brain extracts and extracts prepared from the mouse pituitary cell line αT3, in which CLIM cofactors are expressed to high levels (Ostendorff et al., 2002). The appearance of a band in the zebrafish brain extract migrating at a similar position as mouse CLIM proteins demonstrates that our antiserum recognizes zebrafish CLIM cofactors (Fig. 1A). Using this antiserum, we next investigated CLIM expression in developing zebrafish embryos in immunohistochemical experiments. We detected widespread CLIM protein expression in the developing zebrafish eye, brain and spinal cord at 24 h post-fertilization (hpf) (Fig. 1B), confirming the previously described mRNA expression patterns of CLIM/Ldb cofactors (Toyama et al., 1998). However, CLIM protein was not homogeneously expressed because we detected higher levels of CLIM protein expression in the developing eye, trigeminal neurons, in the hindbrain and in Rohon Beard (RB) neurons (Fig. 1B). Both trigeminal and RB neurons are sensory neurons that are also labeled by the antibody directed against the Isl-1 class of LIM homeodomain factors. Co-immunohistochemistry with both antisera revealed that CLIM cofactors (red) and proteins of the Isl-1 class (green) are coexpressed (yellow) in trigeminal as well as in RB neurons (Fig. 1C). This coexpression strongly suggests important functions of CLIM proteins in conjunction with Isl LIM-HD factors during development of these cell types.

2.2. Overexpressing dominant-negative CLIM results in an inhibition of eye and MHB development

Choosing zebrafish as a model system to study development allows the ectopic overexpression of proteins by injecting mRNA into early stage embryos. First, we investigated the protein expression levels induced by our in vitro produced mRNAs in injected zebrafish embryos. Injecting an mRNA encoding a nuclear localization signal fused to a Myc-tag resulted in an efficient and widespread nuclear expression of the encoded protein as revealed by whole mount immunohistochemical experiments using a specific FITC-labeled Myc-antibody on 24 hpf embryos (Fig. 2A,B). However, although staining of injected zebrafish embryos showed strong expression in most cells of the developing embryo, the penetrance of the obtained phenotypes was not 100%, indicating a variable degree of mosaic protein expression.

To investigate functions of CLIM cofactors during zebrafish development, we then ectopically overexpressed a Myc-epitope tagged dominant-negative version of the CLIM molecule that contains the highly conserved LIM-interaction domain (LID), which confers high-affinity protein interactions with LIM domains, fused to a nuclear localization sequence (Fig. 2C,D). It has been previously shown that overexpressing the DN-CLIM mutant protein results in a competition with wild-type CLIM molecules for binding to LIM domains of LIM-HD proteins (Bach et al., 1999). The phenotypes of DN-CLIM injected embryos were investigated using differential interference contrast optics (Fig. 3A,B) to study live embryos, or immunohistochemistry with a tubulin antibody to better visualize the nervous system and its neuronal projections (Fig. 3C–H). These investigations revealed that in DN-CLIM overexpressing animals both eye (red arrows) and MHB (blue arrows) development was inhibited. In 90% (18 of 20 randomly selected embryos) of DN-CLIM injected animals the eyes were either missing completely or were significantly reduced in size (Fig. 3A–D, red arrows), demonstrating a critical involvement of this cofactor family for the development of this organ. Development of the MHB region (blue arrows) was severely impaired in 70% (11 of 16) of the DN-CLIM overexpressing embryos (Fig. 3E,F). The phenotypes were specific for DN-CLIM mRNA injections because embryos overexpressing the Myc-NLS protein were indistinguishable from wild-type animals (Fig. 3A,C). Furthermore, despite an apparent loss of large brain structures in DN-CLIM overexpressing animals, the remaining anterior CNS appeared normal as evidenced by normal positions of the dorso-ventral diencephalic tract and the posterior commissure in anti-tubulin stained embryos (Fig. 3G,H, black and red arrows, respectively), the normal appearance of the otic vesicles (Fig. 3A,B, black arrows) and similar expression patterns of anterior markers (see below). The primordium of the lateral line had migrated to trunk segment 4.6 ± 0.32 SEM in controls and 4.1 ± 0.28 in experimentals, values not significantly

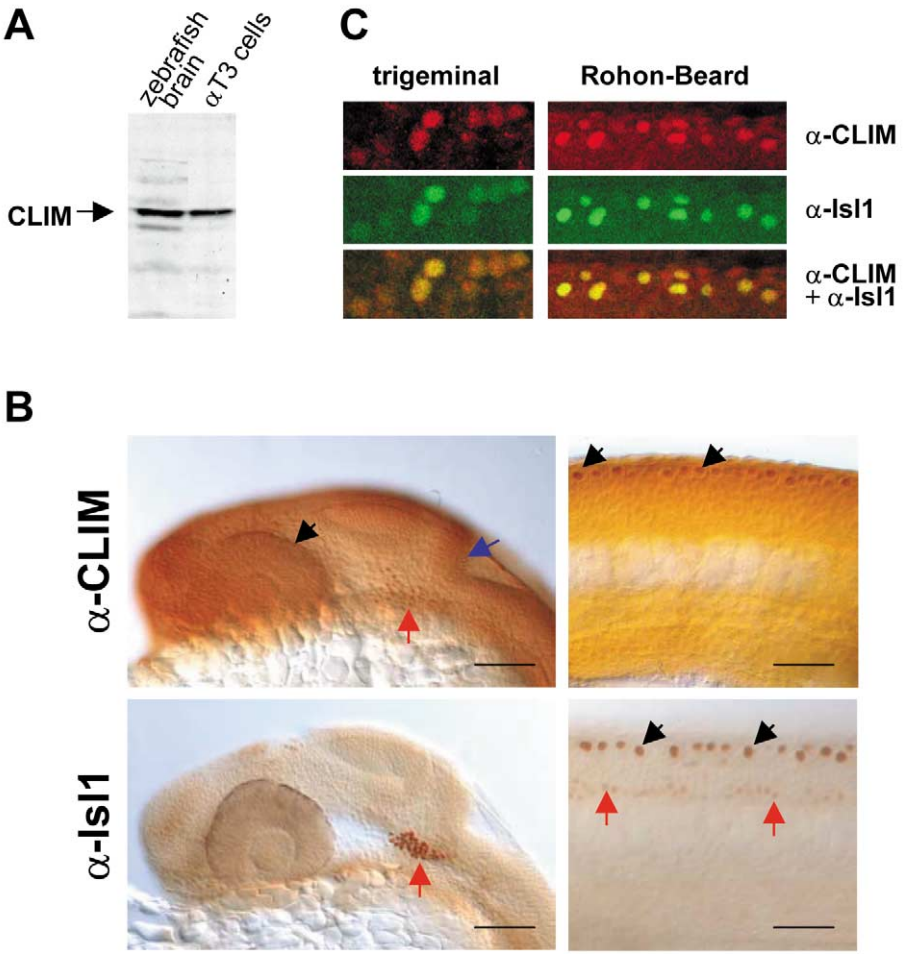

Fig. 1. Comparison of CLIM cofactor expression with Isl LIM-HD proteins in zebrafish embryos (24 hpf) in whole mount immunohistochemistry. (A) Western blot on total cell extracts from adult zebrafish whole brain tissue and the mouse αT3 pituitary cell line using a specific CLIM antiserum. (B) Head regions (left pictures) and trunk regions (right pictures) of embryos stained with CLIM and Isl1 antisera are shown (upper and lower panels, respectively). Selected and specifically stained embryonic regions are indicated with arrows. Head regions: The CLIM antiserum labels many embryonic structures, among which are developing eyes, trigeminal ganglia and hindbrain (indicated by black, red, and blue arrows, respectively). Strongest Isl expression was seen in trigeminal ganglia (red arrow). Trunk regions: CLIM antiserum labels many embryonic structures, among which are nuclei of RB neurons (black arrows). Isl1 antibodies label nuclei of RB neurons (black arrows) and motor neurons (red arrows). The scale bars represent 60 μm. (C) Double immunohistochemistry using the CLIM (red) and Isl1 (green) antisera under a confocal microscope, shows coexpression (yellow) of CLIM cofactors with homeodomain proteins of the Isl class in trigeminal neurons (left) and RB neurons (right).

different from each other. This indicates that general development proceeded normally in the experimental animals.

To investigate the eye and MHB phenotypes in more detail we subsequently analyzed the changes in gene expression caused by DN-CLIM overexpression at 24 hpf (Fig. 4) and 14 hpf embryos (Fig. 5). Comparing gene markers expressed in the eye shows that RxC (Mathers et al., 1997; Chuang and Raymond, 2001) and Six3.1 (Seo et al., 1998) were not expressed in the developing eye in DN-CLIM overexpressing animals, whereas expression of markers in other body regions did not seem to be impaired (Fig. 4A–D). The fact that expressions of Otx2 (Mori et al., 1994) in the midbrain and RxB (Mathers et al., 1997) in the ventral forebrain were readily detectable in DN-CLIM overexpressing animals (Fig. 4E–H) suggests that the overall patterning of both structures is grossly normal. However, analyzing gene markers expressed in the MHB region showed that the development of this structure was strongly inhibited by our DN-CLIM overexpressions. Expression of Eng2 (Fjose et al., 1992), Ephrin-A5b (Picker et al., 1999), PaxB (Krauss et al., 1991), FGF-8 (Fürthauer et al., 1997) and Wnt-1 (Molven et al., 1991) disappeared in the MHB region of DN-CLIM overexpressing animals, whereas expression in other embryonic structures seemed unaffected (Fig. 4I–R). A dorsal midline defect in the DN-CLIM animals is suggested by the fact that PaxB expression in the anterior commissure region was interrupted across the midline (Fig. 4N, blue arrows). The absence of Wnt-1 expression along the dorsal midbrain midline seems to confirm this observation (Fig. 4R, blue arrow).

In DN-CLIM overexpressing embryos we failed to detect RxC expression at 14 hpf (Fig. 5A,B), suggesting a lack of

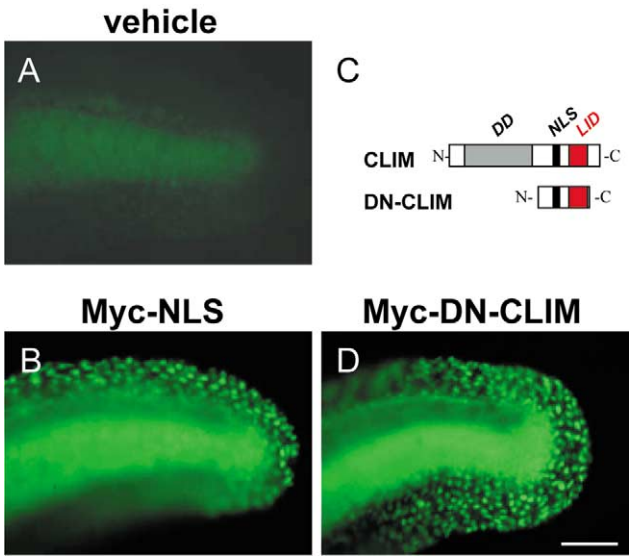

Fig. 2. Embryonic expression of injected mRNA in the tail as detected with α-Myc staining at 24 hpf. (A) A vehicle-injected zebrafish embryo is shown. (B) Nuclear expression of a control protein containing six Myc epitopes fused to a nuclear localization sequence in zebrafish embryos. (C) Schematic representations of CLIM full length and the dominant-negative CLIM molecule (DN-CLIM) which contains the nuclear localization sequence (NLS, in black) and the LIM interaction domain (LID, in red) of CLIM1. The dimerization domain (DD) that is deleted in DN-CLIM is indicated in gray. (D) Nuclear expression of the Myc-DN-CLIM protein following mRNA injection. The scale bar represents 60 μm in A,B,D.

eye primordia caused by our injections. Unlike 24 hpf embryos, initial Eng2 expression was detected, albeit weaker, in DN-CLIM animals at 14hpf (Fig. 5C,D). DN-CLIM overexpression resulted also in a downregulation of FGF-8 expression specifically in the MHB, whereas expression in an anterior expression domain, rhombomeres 3 and 5, somites and a posterior expression domain was not affected (Fig. 5E,F and data not shown). These results are consistent with a disturbance of marker gene expression at the maintenance level.

2.3. CLIM cofactors are required for axonal outgrowth of specific neurons

Since we detected highest CLIM cofactor expression in trigeminal ganglia and RB sensory neurons we investigated potential roles of this class of cofactors for the development of both types of neurons. The analysis of axon trajectories was carried out on whole mounted zebrafish embryos (24 hpf) that were stained using an anti-tubulin antibody. The tubulin antibody labels most embryonic neurons and their neurites. Whereas peripheral axons from trigeminal ganglia normally grow in a defasciculated way to innervate various skin regions (Fig. 6A), axons of trigeminal ganglia in DN-CLIM-injected embryos exhibited strong fasciculation (Fig. 6B). The number of peripheral axon fascicles was reduced by approximately 65% in experimental embryos, compared to Myc-NLS-injected controls (Fig. 6K). While peripheral axons were greatly reduced in number, tubulin-labeled neuronal somata had developed normally in the ganglion and the central projections of these neurons seemed unaffected. Analysis of the RB neurons in DN-CLIM-injected animals revealed that more than 60% of the peripheral axons of this class of neurons normally projecting into the skin were lacking, whereas animals injected with the Myc-NLS-tag showed normal outgrowth of axons (Fig. 6C–F,K).

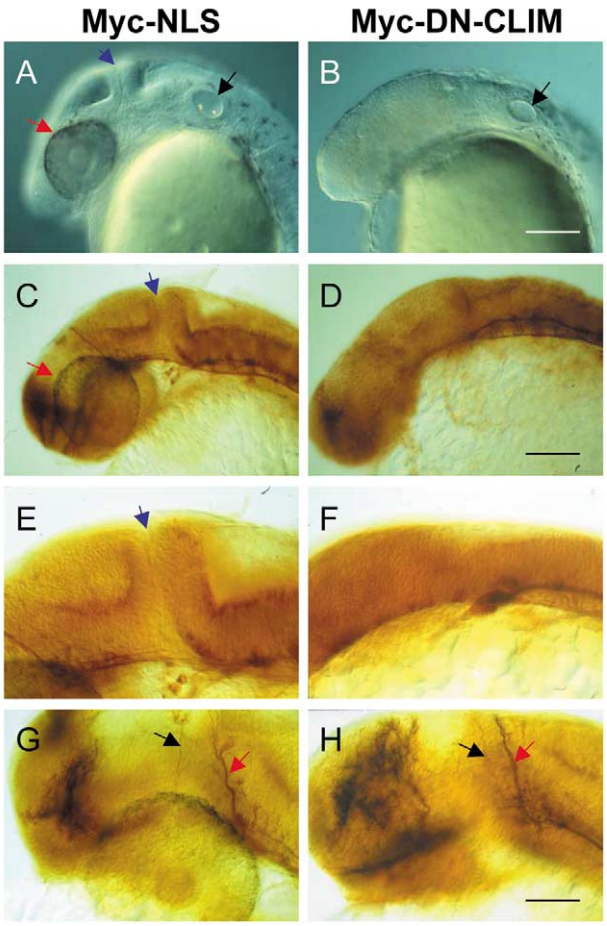

Fig. 3. DN-CLIM inhibits eye development and disturbs the formation of the MHB. Head regions of embryos injected with Myc-NLS mRNA (A,C,E,G), or with the Myc-DN-CLIM mRNA (B,D,F,H). Eye, MHB and otic vesicle are indicated by red, blue and black arrows, respectively (A–F). Live embryos using differential interference contrast (DIC) optics (A,B) and embryos stained with α-tubulin (C–H) are shown. (A) The head region of a live control embryo visualized using DIC optics. (B) The head region of a live embryo injected with DN-CLIM mRNA visualized by using DIC optics. Note that the eyes and the MHB are missing. The scale bar represents 250 μm in A,B. (C) The head region of a control embryo injected with Myc-NLS mRNA is shown. (D) The head region of an embryo injected with DN-CLIM mRNA is shown. Note that the eyes are completely missing. The scale bar represents 200 μm in C,D. (E) MHB in Myc-NLS mRNA injected control animals. (F) MHB in Myc-DN-CLIM mRNA injected embryos. Note the impairment of boundary formation and the overall diminution of cell mass. (G,H) Normal development of axons in the dorso-ventral diencephalic tract (black arrow) and the posterior commissure (red arrow) in anterior head regions is observed in both Myc-NLS and Myc-DN-CLIM mRNA injected animals. The scale bar represents 120 μm in E–H.

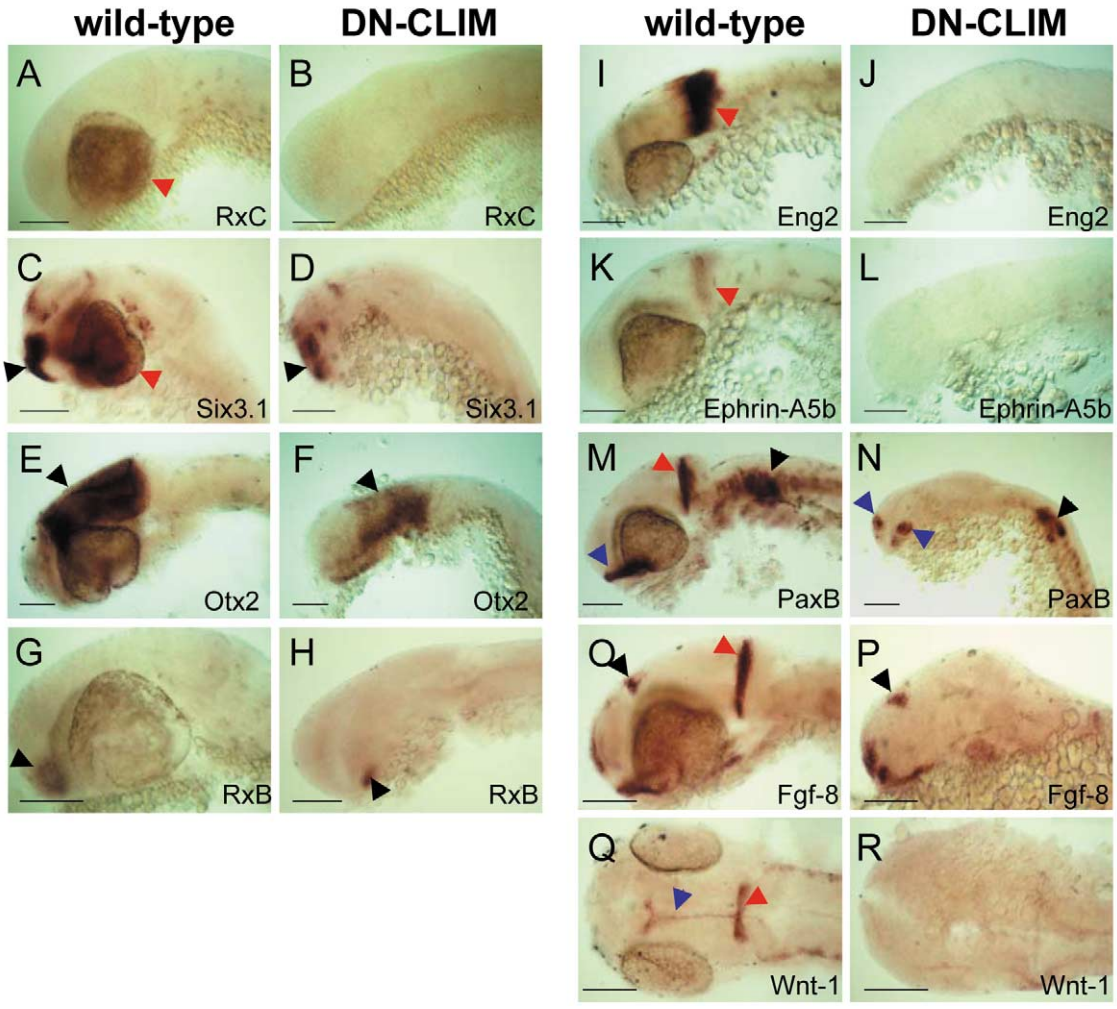

Fig. 4. Analysis of gene markers expressed in eye and MHB by whole mount in situ hybridizations on zebrafish embryos (24 hpf). Wild type (A,C,E,G,I,K,-M,O,Q) and Myc-DN-CLIM overexpressing animals (B,D,F,H,J,L,N,P,R) are shown. Scale bars represent 180 μm. (A) Untreated embryos stained with the RxC probe showed specific staining in the eye (red arrow). (B) Eyeless DN-CLIM overexpressing animals lacked RxC staining. (C) Untreated embryos stained with the Six3.1 probe showed specific labeling in eye and anterior head regions (red and black arrows, respectively). (D) DN-CLIM overexpressing animals lacked Six3.1 staining in the eye, whereas stainings in anterior head regions were still detectable (black arrow). (E) Untreated embryos stained with the Otx2 probe showed specific staining in the dorsal midbrain and diencephalon (black arrow). (F) In DN-CLIM overexpressing animals Otx2 staining was weaker, but still detectable (black arrow). (G) Untreated embryos stained with the RxB probe showed specific staining in ventral forebrain regions (black arrow). (H) Normal RxB staining in ventral forebrains of DN-CLIM overexpressing animals (black arrow). (I) Untreated embryos stained with the Eng2 probe showed specific staining in the MHB (red arrow). (J) DN-CLIM overexpressing animals lacked Eng2 staining. (K) Untreated embryos stained with the Ephrin-A5b probe showed specific staining in the MHB (red arrow). (L) DN-CLIM overexpressing animals lacked Ephrin-A5b staining. (M) Wild-type expression of PaxB in the otic vesicle, MHB and anterior commissure region (black, red and blue arrow, respectively). (N) Lack of PaxB staining in the MHB region in an animal shown from an oblique angle. PaxB expression in the otic vesicle (black arrow) and the anterior commissure region (blue arrows) was still detectable. Note that anterior PaxB staining is interrupted across the midline. (O) Fgf-8 is expressed in the MHB and the epiphysis (red and black arrow, respectively) among other embryonic regions in wild-type animals. (P) DN-CLIM overexpressing animals lack Fgf-8 staining in the MHB, whereas staining in other regions (i.e. epiphysis, black arrow) seems unaffected. (Q) Dorsal view of a wild type embryo stained with a Wnt-1 probe. The MHB (red arrow) and the dorsal midline are stained (blue arrow). (R) Loss of Wnt-1 staining in DN-CLIM injected animals is apparent.

Again, this was due to an impairment of the outgrowth of peripheral axonal projections, since the tubulin-labeled cell bodies of this cell type were present in their normal position in the dorsal spinal cord (Fig. 6G,H) and the central projections in the dorsal longitudinal fascicle were not affected. Counting somata of RB cells in trunk segments 7–14 actually revealed an increase of 34% in the number of somata compared to NLS-injected controls. Furthermore, more than 60% of the segments showed severely impaired axonal outgrowth of ventral motor neurons along their midsegmental pathway to the ventral somite upon overexpression of DN-CLIM (Fig. 6I–K). This demonstrates that CLIM function is needed for axonal outgrowth of several types of neurons. Indeed, about half of the DN-CLIM-injected animals showed almost complete loss of peripheral axons from these types of neurons. The described phenotypes in

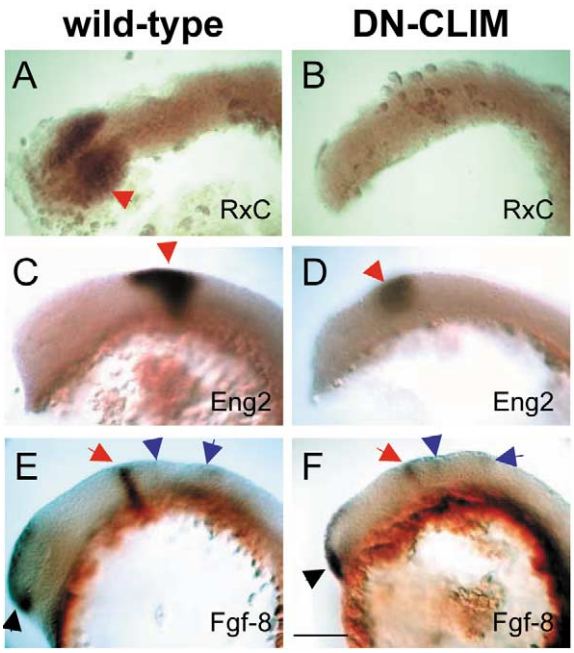

Fig. 5. Analysis of gene markers by whole mount in situ hybridizations of 14 hpf zebrafish embryos. Wild-type (A,C,E) and Myc-DN-CLIM overexpressing animals (B,D,F) are shown. The scale bar represents 120 μm (A–F). (A) Dorsal view of untreated embryos stained with the RxC probe showed specific staining in the developing eyes (red arrow). (B) DN-CLIM overexpressing animals lacked RxC staining, presumably due to the loss of this organ. (C) A lateral view of an untreated embryo stained with the Eng2 probe shows specific staining in the MHB region (red arrow). (D) A DN-CLIM overexpressing animal shows weaker but detectable levels of Eng2 in the MHB region (red arrow). (E) Lateral view of a wild type embryo stained with the Fgf-8 probe showing specific staining in an anterior expression region (black arrow) and MHB (red arrow) and lower expression in rhombomeres 3 and 5 (blue arrows). (F) Fgf-8 expression in DN-CLIM overexpressing animals appears normal in the anterior expression region (black arrow) and rhombomeres 3 and 5 (blue arrows), whereas expression levels were weaker but detectable in the MHB region (red arrow).

these neurons were specific, because other axons, e.g. the posterior commissure and the dorso-ventral diencephalic tract (Fig. 3G,H) or in the posterior lateral line nerve (not shown), were not affected by the DN-CLIM overexpression. Interestingly, the involvement of LIM-HD proteins in the development of neuronal projections has previously been noted in both *Drosophila* and mice (Thor et al., 1999; Sharma et al., 1998), suggesting that our DN-CLIM overexpression results in an inhibition of specific LIM-HD protein activity necessary for axon growth in specific neurons. Experiments aimed to rescue the DN-CLIM phenotype by coinjecting mRNA encoding Myc-tagged full-length CLIM1 or CLIM2 were not successful, presumably due to a short half-life of full-length CLIM proteins. This was evidenced by the fact that Myc-CLIM full-length protein was well detectable in 5 hpf zebrafish embryos but never at 14 hpf or beyond, even when increased amounts of mRNA were injected (up to 5 ng; data not shown). In comparison, Myc-DN-CLIM was still readily detectable at 24 hpf (Figs. 2D and 6D).

2.4. CLIM cofactor inhibition results in deregulated neuronal expression of isl genes

LIM-HD protein concentrations have been shown to be affected by proteasomal degradation during *Drosophila* wing development (Weihe et al., 2001). In addition, we have previously demonstrated that CLIM proteins can protect nuclear LIM proteins from ubiquitination and that this protection was dependent on the presence of the LID domain (Ostendorff et al., 2002). Therefore we investigated whether DN-CLIM overexpressing animals might exhibit altered Isl protein expression. Indeed, immunodetection with Isl antibodies at stage 24 hpf revealed a wider expression of Isl-related LIM-HD proteins in different neuronal cell types of DN-CLIM overexpressing animals when compared to wild type (Fig. 7A–D). Stronger Isl-expressing cells are seen in cell types around the otic vesicle, some of which are normally only weakly labeled by this antibody (Korzh et al., 1993), e.g. the anterior and posterior lateral line ganglia (Fig. 7A–D). In trunk regions of DN-CLIM overexpressing animals, Isl-positive cells were observed in intermediate neural tube regions between the RB and motor neurons (Fig. 7C,D) where interneurons are located. These results demonstrate that the CLIM cofactor family is involved in the regulation of Isl protein expression in neurons.

3. Discussion

The LIM domain-binding CLIM cofactors are highly conserved from *Drosophila* to human (Bach, 2000). The formation of CLIM/LIM-HD complexes has been shown to be critical for at least some of the in vivo functions of LIM-HD genes (Morcillo et al., 1997; Bach et al., 1999; Milán and Cohen, 1999; van Meyel et al., 1999, 2000; Rincon-Limas et al., 2000). To investigate the role of CLIM cofactors we have overexpressed a previously characterized dominant-negative version of CLIM fused to a Myc epitope-tag (DN-CLIM) early during zebrafish embryogenesis. It has been demonstrated that DN-CLIM, which contains the LIM-interaction domain (LID), is able to compete with wild type CLIM molecules for LIM domain binding (Bach et al., 1999). The high sequence conservation of zebrafish CLIM molecules, in particular the LID, which is almost identical to that of CLIM proteins originating from other vertebrate species (Toyama et al., 1998), strongly suggests that overexpression of DN-CLIM inhibits the association of all four zebrafish CLIM versions with LIM domains and, as a consequence, disrupts LIM-HD activity.

Using a specific anti-CLIM antiserum (Ostendorff et al., 2002), our immunohistochemical results show that members of this class of cofactors are widely expressed in many tissues and cell types of known LIM-HD expression including the developing eye, MHB and specific neurons of the CNS and PNS. Consistent with this pattern of expression we

show that overexpression of the DN-CLIM protein early during zebrafish development results in a potent inhibition of eye formation with the disappearance of all gene markers tested, in both 14 and 24 hpf embryos. These results match well with previously obtained results in mice in which the deletion of the LIM-HD gene Lhx2 resulted in a phenotype that showed a severe inhibition of eye development (Porter et al., 1997). Furthermore, DN-CLIM is also able to disrupt the proper formation of the MHB, a structure in which several LIM-HD proteins are prominently expressed (Bach et al., 1997). In DN-CLIM-injected embryos the expression of both early and late MHB gene markers at 24 hpf was abolished. The absence of marker gene expression in both developing eye and MHB strongly suggests that these structures are completely missing at 24 hpf. However, because MHB formation initially occurs in DN-CLIM overexpressing animals, as indicated by the onset of Eng2 and Fgf-8 gene expression at 14 hpf, an impairment at the level of cell and/or transcriptional maintenance seems likely. It remains unclear whether this is also the case for the observed inhibition of eye development. It is of interest to note that gene deletions of the Lhx1 gene resulted in an inhibition of the development of anterior head structures (Shawlot and Behringer, 1995), a phenotype that is not paralleled upon DN-CLIM overexpression. One possible explanation for this discrepancy may be that high endogenous CLIM levels during early zebrafish development may require DN-CLIM expression levels higher than those obtained by our overexpressions.

We have shown that the overexpression of DN-CLIM early during zebrafish development strongly inhibits peripheral axon outgrowth of specific sensory neurons. These data match well with our immunohistochemical data and the previously published expression patterns of Isl-1 and CLIM cofactors (Korzh et al., 1993; Toyama et al., 1998). However, the underlying expression patterns of factors recognized by the antibodies used in this study are probably more complex, since both antisera recognize more than one protein of their respective class. Interestingly, the inhibition of axonal outgrowth in sensory neurons is specific for peripheral axons, since their cell somata, together with the central projections, were still present. The reasons for the observed increase of RB neurons in DN-CLIM overexpressing animals are not clear but may hint towards roles of CLIM cofactors in the proliferation/establishment of cell numbers of specific neuronal cell types.

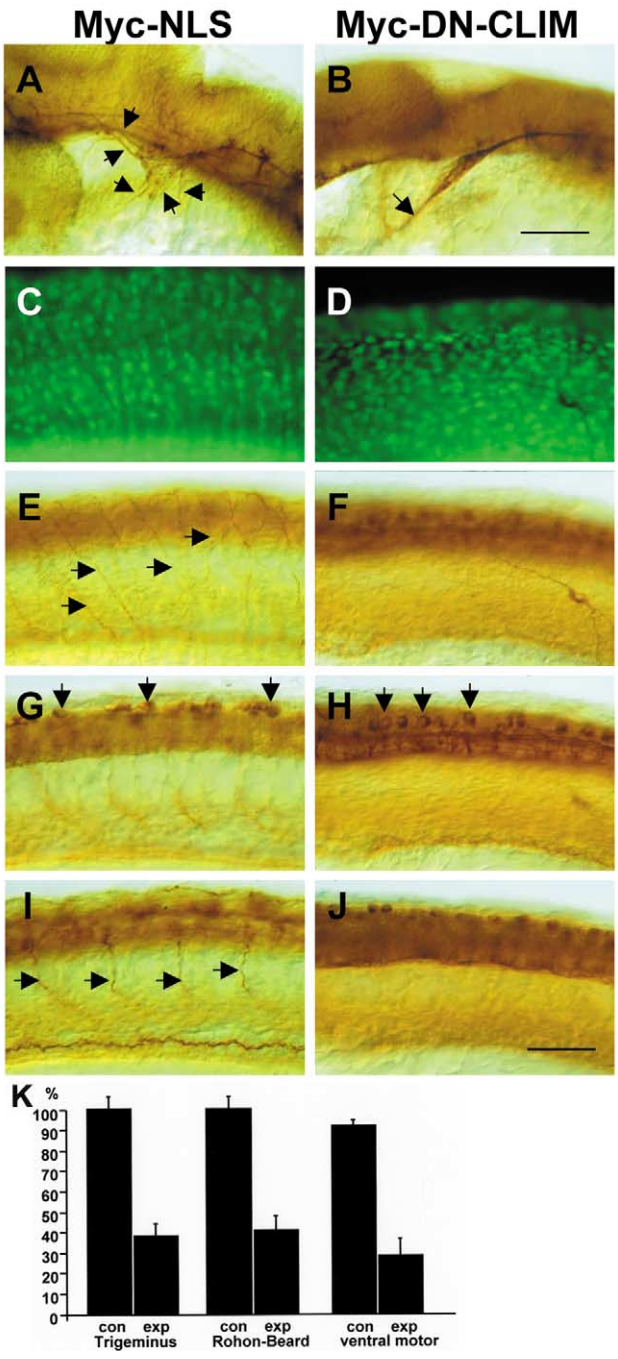

Fig. 6. DN-CLIM inhibits the development of peripheral axons. Myc-NLS (A,C,E,G,I) or Myc-DN-CLIM (B,D,F,H,J) encoding mRNAs were injected into zebrafish embryos. Embryos (24 hpf) are shown after whole mount immunohistochemistry using α-Myc (C,D) or α-tubulin antisera (A,B,E–J). A and B show the embryonic head regions whereas trunk regions of the same two embryos at different focal planes are shown in C,E,G,I and D,F,H,J, respectively. (A,B) Trigeminal ganglia of injected embryos are shown. Arrows point at peripheral axon fascicles. Note that in the DN-CLIM-injected animals peripheral axons form only one tight bundle. The scale bar represents 120 μm. (C,D) Injected mRNAs are expressed in the embryonic regions shown in E-J as detected by Myc-immunofluorescence. (E,F) Peripheral axonal projections of RB neurons are present in controls but are almost completely absent in DN-CLIM injected animals. Individual fascicles are indicated by arrows. A ventrally displaced RB neuron which is not an effect of DN-CLIM overexpression but used as a focus reference point is seen in F. (G,H) Cell bodies of RB neurons are pointed out by arrows in both panels. (I,J) Axonal projections of motor neurons are indicated by arrows in Myc-NLS-injected controls, but are missing in DN-CLIM-injected experimental animals. The scale bar represents 80 μm in C–J. (K) Percentage of axon fascicles in Myc-NLS-injected control (con) and DN-CLIM-injected (exp) embryos is shown ($n = 20$ embryos). The numbers of peripheral axons/axon fascicles are strongly reduced in trigeminal, RB and motor neurons.

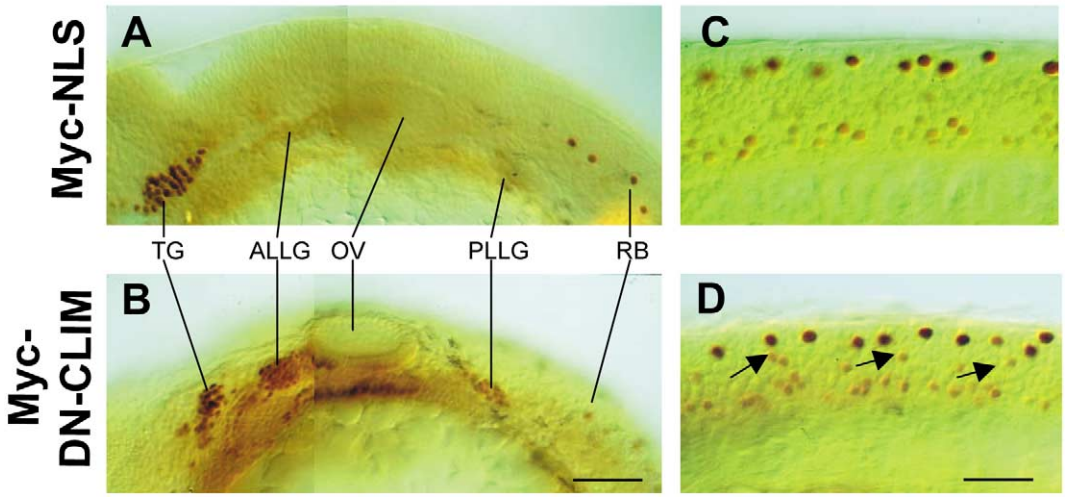

Fig. 7. Injection of DN-CLIM leads to increased levels of Isl LIM-HD proteins in specific neuronal cell types. Embryos are stained with the α-Isl1 antibody at 24 hpf. Anterior regions of Myc-NLS-injected (A) and Myc-DN-CLIM-injected (B) embryos are shown. (C,D) Trunk region showing Isl1-staining in cells (arrows) located in areas where interneurons reside. The scale bars represent 120 μm in A,B and 40 μm in C,D. ALLG, anterior lateral line ganglion; OV, otic vesicle; PLLG, posterior lateral line ganglion; RB, Rohon Beard neurons; TG, trigeminal ganglion.

LIM-HD transcription factors have been shown to be essential for the development of motor neurons (Jurata et al., 2000). In agreement with these data, we show that the overexpression of DN-CLIM specifically inhibits axonal outgrowth of motor neurons. Since immunohistochemical experiments using Isl antiserum revealed the presence of at least some motor neurons, it is likely that, as observed in sensory neurons, axonal outgrowth is specifically inhibited. Again, the phenotype observed in motor neurons matches well with the finding that LIM-HD proteins have been shown to regulate axonal pathfinding of motor neurons (Sharma et al., 1998; Thor and Thomas, 1997; Thor et al., 1999). However, in contrast to the trigeminal or RB neurons we did not detect particularly high CLIM cofactor concentrations in motor neurons (Fig. 1B, upper right panel). This discrepancy may be explained by the fact that four different CLIM cofactors exist in zebrafish and that in the spinal cord at 24 hpf only the mRNA encoding Ldb1 is expressed at high levels, whereas in other embryonic regions at least three CLIM members display strong overlapping mRNA expression (Toyama et al., 1998). Furthermore, our CLIM antiserum may not display the same binding affinity for each of these proteins. The results obtained by the analysis of our DN-CLIM overexpressing animals match well and are complementary to results obtained by analyzing phenotypes of specific Isl-LIM domain-overexpressing zebrafish embryos (Segawa et al., 2001).

Concerning the molecular mechanisms through which DN-CLIM overexpression affects development, it is likely that the function of LIM domains on LIM-HD proteins is inhibited by their stable association with DN-CLIM molecules. Such a ‘locked’ association is probably due to both the high affinity binding of the LIM interaction domain LID with LIM domains and an increased stability of the DN-CLIM/LIM-HD complex. The occupation of LIM domains by DN-CLIM is predicted to block protein interactions resulting in disturbances of LIM-HD function on multiple levels. DN-CLIM competition with endogenous CLIM cofactors for LIM domains will block the formation of CLIM/LIM-HD protein complexes (Bach et al., 1999) which are believed to be crucial for the exertion of the in vivo LIM-HD function (Milán and Cohen, 1999; van Meyel et al., 1999). Previous work has shown that CLIM cofactors regulate the transcriptional activity conferred by LIM-HD proteins (Bach et al., 1997; Jurata and Gill, 1997; Mochizuki et al., 2000). Therefore, a disturbance of the regulation in the gene expression controlled by LIM-HD proteins is expected at the transcriptional level in DN-CLIM overexpressing embryos, in addition to a disruption of other biological functions in which a CLIM/LIM-HD complex may be involved. Since other cofactors recognizing LIM domains of LIM-HD proteins have been identified, e.g. RLIM and SLB (Bach et al., 1999; Howard and Maurer, 2000), that influence the transcriptional activation mediated by LIM-HD proteins, it is likely that DN-CLIM also inhibits their association with LIM-HD proteins, thereby possibly interfering with yet other LIM-HD functions. Furthermore, because CLIM cofactors have been reported to interact not only with LIM-HD factors but also with homeodomain transcription factors of the bicoid class (Bach et al., 1997; Torigoi et al., 2000), we cannot exclude the possibility that an inhibition of these transcriptional regulator proteins by DN-CLIM contributes to the observed phenotypes.

The lack of the dimerization domain in the DN-CLIM molecule led to a dramatic increase in protein detectability when compared with full-length CLIM1 or CLIM2. Since the dimerization domain has been demonstrated to mediate the protein interactions with the ubiquitin ligase RLIM (Ostendorff et al., 2002), it is tempting to speculate that RLIM-like molecules play important roles in the observed

instability of full-length CLIM molecules during zebrafish development. Indeed, in contrast to its full-length counterpart, DN-CLIM protein, lacking the dimerization domain, is not polyubiquitinated by RLIM in vitro (Ostendorff, H.P., Bach, I., unpublished data).

We also detected increased levels of Isl LIM-HD members in neuronal cell types that normally express low levels of these proteins, e.g. the anterior and posterior lateral line ganglia, the epiphysis and interneuron subtypes of the spinal cord (Fig. 7; Korzh et al., 1993). This result suggests further roles of CLIM cofactors in conjunction with LIM-HD factors. In this context it has been recently observed in *Drosophila* that the protein levels of the LIM-HD factor Apterous is regulated during development by the 26S proteasome (Weihe et al., 2001). Furthermore, we have recently shown that CLIM cofactors can protect LIM proteins from ubiquitination mediated by the ubiquitin protein ligase RLIM and that sequences located on the DN-CLIM molecule are sufficient for this protection (Ostendorff et al., 2002). Therefore, the increased levels of Isl protein expression observed in different neuronal cell populations is likely to be due to a DN-CLIM-mediated protection from proteasomal degradation. Taken together, our results demonstrate multiple functions of CLIM cofactors in organ development and the development of peripheral axonal projections.

4. Material and methods

4.1. Animals

Zebrafish embryos were collected from our breeding colony according to standard procedures (Westerfield, 1989). Embryos were staged in hours post-fertilization (hpf) at standard temperature (28.5 °C), which was deduced from determining the segmental position of the lateral line primordium (Kimmel et al., 1995).

4.2. Western blots

A Western blot on total extracts of adult zebrafish brain and αT3 cells, a cell line derived from gonadotrope cells of the mouse pituitary (Windle et al., 1990) was carried out as described previously (Sambrook et al., 1989). The blot was hybridized with a 1:5000 dilution of the CLIM antiserum (Ostendorff et al., 2002) and Protein A horseradish peroxidase (HRP; BioRad) was used to visualize specific bands.

4.3. Injection of mRNAs into fertilized eggs

Previously described Myc epitope-tagged DN-CLIM, CLIM1 or CLIM2 in the CS2-MT plasmid (Bach et al., 1997, 1999) or control CS2-MT-NLS plasmid that contains a nuclear localization sequence was in vitro transcribed to produce mRNAs using the mMessage mMachine kit (Ambion) and Sp6 RNA polymerase according to the manufacturers instructions. Preparations of myc-tagged mRNAs were injected into the yolk of 1–4 cell stage embryos as previously described (Roos et al., 1999). Briefly, approximately 2 nl of mRNA (100–250 ng/μl) containing 0.5% RDA was pressure injected. Animals were allowed to develop to 14 or 24 hpf, at which point they were processed for immunohistochemistry. Survival rates between injected and uninjected embryos were indistinguishable.

4.4. Immunohistochemistry

The antibodies used in this study were: CLIM antiserum (Ostendorff et al., 2002), Islet-1 40.2D6 monoclonal antibody (Developmental Studies Hybridoma Bank, Iowa City, IA) recognizing Isl-1 and Isl-2, FITC-conjugated Myc antibody 9E10 (Covance, Princeton, NJ) and anti-acetylated tubulin (Sigma). Immunohistochemistry on whole-mounted embryos has previously been described (Becker et al., 2001). Briefly, embryos were dechorionated, deeply anesthetized in 0.1% aminobenzoic acid ethyl methyl ester in PBS, fixed in 4% paraformaldehyde, incubated with primary antibodies overnight and with HRP-coupled secondary antibodies again overnight. Labeling was detected with diaminobenzidine as a substrate for the HRP. Replacing the primary antibody with non-immune IgGs did not result in any labeling. To detect the Myc-epitope in embryos which were processed for tubulin labeling, these embryos were incubated with the fluorescein isothiocyanate-coupled anti-myc antibody again overnight after the tubulin labeling had been developed. Embryos were washed and directly mounted in glycerol.

4.5. In situ hybridizations

Non-radioactive detections of mRNAs in 14 and 24 hpf whole-mount larvae were performed as previously published (Becker et al., 2001). Briefly, whole embryos were incubated with the digoxygenin-labeled RNA-probe at 55 °C overnight, and washed extensively at 55 °C. The labeling reaction was performed using the Sp6 Megascript kit (Ambion). The hybridized probes were detected using an alkaline phosphatase-coupled anti-digoxygenin antibody (Roche, Mannheim, Germany). The sense probes served as negative controls and did not show any label.

4.6. Quantification of axons and cells in tubulin labeled embryos

Axons of trigeminal, Rohon Beard and caudal primary motor neurons were quantified in 20 randomly selected embryos from the NLS-injected control and DN-CLIM injected groups. Axon outgrowth from trigeminal ganglia was quantified by counting the number of individual fascicles directly at the point at which the fascicles emanated from the ganglion. Only the upper ganglion was analyzed, due to its better visibility in embryos that were whole-mounted on their sides (Fig. 6A,B). We quantified RB

somata and axons, as well as axons of caudal primary motor neurons in trunk segments 7–14, since these were fully developed and not obscured by yolk droplets. RB somata were counted on both sides of the embryo, while primary branches of peripheral axons were counted in the most dorsal aspect of the upper side only (Fig. 6E–H). Axons of caudal primary motor neurons were counted on both sides of the embryo (Fig. 6I,J). Numbers of axons were expressed as percent of controls in Fig. 6K, with the exception of axons of the caudal primary motor neurons that were expressed as percent of the expected value of 16 axons for 8 trunk segments analyzed.

Acknowledgements

We thank Drs. C. Brennan, M. Hammerschmidt and C. Thisse for cDNA probes, Dr. C. Kintner for the pCS2MT vectors, B. Viehweger for technical assistance and Dr. M. Schachner for critically reading the manuscript and for support. H.P.O. was a fellow of the Graduiertenkolleg 255 of the University of Hamburg and I.B. is a Heisenberg scholar of the Deutsche Forschungsgemeinschaft (DFG). This work was supported by grants from the DFG to I.B. and T.B.

References

Agulnick, A.D., Taira, M., Breen, J.J., Tanaka, T., Dawid, I.B., Westphal, H., 1996. Interactions of the LIM-domain-binding factor Ldb1 with LIM homeodomain proteins. Nature 384, 270–272.

Bach, I., 2000. The LIM domain: Regulation by association. Mech. Dev. 91, 5–17.

Bach, I., Carrière, C., Ostendorff, H.P., Andersen, B., Rosenfeld, M.G., 1997. A family of LIM domain interacting cofactors confer transcriptional synergism between LIM and Otx homeoproteins. Genes Dev. 11, 1370–1380.

Bach, I., Rodriguez-Esteban, C., Carrière, C., Bhushan, A., Krones, A., Rose, D.W., Glass, C.K., Andersen, B., Ispizúa Belmonte, J.C., Rosenfeld, M.G., 1999. RLIM inhibits functional activity of LIM homeodomain transcription factors via recruitment of the histone deacetylase complex. Nat. Genet. 22, 394–399.

Becker, T., Becker, C.G., Schachner, M., Bernhardt, R.R., 2001. Antibody to the HNK-1 glycoepitope affects fasciculation and axonal pathfinding in the developing posterior lateral line nerve of embryonic zebrafish. Mech. Dev. 109, 37–49.

Chuang, J.C., Raymond, P.A., 2001. Zebrafish genes rx1 and rx2 help define the region of forebrain that gives rise to retina. Dev. Biol. 231, 13–30.

Dawid, I.B., Chitnis, A.B., 2001. LIM homeobox genes and the CNS: a close relationship. Neuron 30, 301–303.

Fjose, A., Njolstad, P.R., Nornes, S., Molven, A., Krauss, S., 1992. Structure and early embryonic expression of the zebrafish engrailed-2 gene. Mech. Dev. 39, 51–62.

Fürthauer, M., Thisse, C., Thisse, B., 1997. A role for FGF-8 in the dorsoventral patterning of the zebrafish gastrula. Development 124, 4253–4264.

Hobert, O., Westphal, H., 2000. Functions of LIM-homeobox genes. Trends Genet. 16, 75–83.

Howard, P.W., Maurer, R.A., 2000. Identification of a conserved protein that interacts with specific LIM homeodomain transcription factors. J. Biol. Chem. 275, 13336–13342.

Jurata, L.W., Gill, G.N., 1997. Functional analysis of the nuclear LIM domain interactor NLI. Mol. Cell. Biol. 17, 5688–5698.

Jurata, L.W., Kenny, D.A., Gill, G.N., 1996. Nuclear LIM interactor, a rhombotin and LIM homeodomain interacting protein, is expressed early in neuronal development. Proc. Natl. Acad. Sci. USA 93, 11693–11698.

Jurata, L.W., Pfaff, S.L., Gill, G.N., 1998. The nuclear LIM domain interactor NLI mediates homo- and heterodimerization of LIM domain transcription factors. J. Biol. Chem. 273, 3152–3157.

Jurata, L.W., Thomas, J.B., Pfaff, S.L., 2000. Transcriptional mechanisms in the development of motor control. Curr. Opin. Neurobiol. 10, 72–79.

Kania, A., Johnson, R.L., Jessell, T.M., 2000. Coordinate roles for LIM homeobox genes in directing dorsoventral trajectory of motor axons in the vertebrate limb. Cell 102, 161–173.

Kimmel, C.B., Ballard, W.W., Kimmel, S.R., Ullmann, B., Schilling, T.F., 1995. Stages of embryonic development of the zebrafish. Dev. Dyn. 203, 253–310.

Korzh, V., Edlund, T., Thor, S., 1993. Zebrafish primary neurons initiate expression of the LIM homeodomain protein Isl-1 at the end of gastrulation. Development 118, 417–425.

Krauss, S., Johansen, T., Korzh, V., Fjose, A., 1991. Expression of the paired box gene pax(zf-b) during early neurogenesis. Development 113, 1193–1206.

Mathers, P.H., Grinberg, A., Mahon, K.A., Jamrich, M., 1997. The Rx homeobox gene is essential for vertebrate eye development. Nature 387, 603–607.

Milán, M., Cohen, S.M., 1999. Regulation of LIM Homeodomain activity in vivo: A tetramer of dLDB and Apterous confers activity and capacity for regulation by dLMO. Mol. Cell 4, 267–273.

Mochizuki, T., Karavanov, A.A., Curtiss, P.E., Ault, K.T., Sugimoto, N., Watabe, T., Shiokawa, K., Jamrich, M., Cho, K.W., Dawid, I.B., Taira, M., 2000. Xlim-1 and LIM domain binding protein 1 cooperate with various transcription factors in the regulation of the goosecoid promoter. Dev. Biol. 224, 470–485.

Molven, A., Njolstad, P.R., Fjose, A., 1991. Genomic structure and restricted neural expression of the zebrafish wnt-1 (int-1) gene. EMBO J. 10, 799–807.

Morcillo, P., Rosen, C., Baylies, M.K., Dorsett, D., 1997. Chip, a widely expressed chromosomal protein required for segmentation and activity of a remote wing margin enhancer in Drosophila. Genes Dev. 11, 2729–2740.

Mori, H., Miyazaki, Y., Morita, T., Nitta, H., Mishina, M., 1994. Different spatio-temporal expressions of three otx homeoprotein transcripts during zebrafish embryogenesis. Brain Res. Mol. Brain Res. 27, 221–231.

Ostendorff, H.P., Peirano, R.I., Peters, M., Schlüter, A., Bossenz, M., Scheffner, M., Bach, I., 2002. Ubiquitination-dependent cofactor exchange on LIM homeodomain proteins. Nature 416, 99–103.

Pfaff, S.L., Mendelsohn, M., Stewart, C.L., Edlund, T., Jessell, T.M., 1996. Requirement for LIM homeobox gene Isl1 in motor neuron generation reveals a motor neuron-dependant step in interneuron differentiation. Cell 84, 309–320.

Picker, A., Brennan, C., Reifers, F., Clarke, J.D.W., Holder, N., Brand, M., 1999. Requirement for the zebrafish mid-hindbrain boundary in midbrain polarisation, mapping and confinement of the retinotectal projection. Development 126, 2967–2978.

Porter, F.D., Drago, J., Xu, Y., Cheema, S.S., Wassif, C., Huang, S.-P., Lee, E., Grinberg, A., Massalas, J.S., Bodine, E., Alt, F., Westphal, H., 1997. Lhx2, a LIM homeodomain gene, is required for eye, forebrain, and definitive erythrocyte development. Development 124, 2935–2944.

Rincon-Limas, D.E., Lu, C.H., Canal, I., Botas, J., 2000. The level of DLDB/Chip controles the activity of the LIM homeodomain protein Apterous: evidence for a functional tetramer complex in vivo. EMBO J. 19, 2602–2614.

Roos, M., Schachner, M., Bernhardt, R.R., 1999. Zebrafish semaphorin Z1b inhibits growing motor axons in vivo. Mech. Dev. 87, 103–117.

Sambrook, J., Fritsch, E.F., Maniatis, T., 1989. Molecular Cloning: A Laboratory Manual, . 2nd EditionCold Spring Harbor Laboratory Press, Cold Spring Harbor, NY.

Segawa, H., Miyashita, T., Hirate, Y., Higashijima, S., Chino, N., Uyemura, K., Kikuchi, Y., Okamoto, H., 2001. Functional repression of Islet-2 by disruption of complex with Ldb impairs peripheral axonal outgrowth in embryonic zebrafish. Neuron 30, 423–436.

Seo, H.C., Drivenes, O., Ellingsen, S., Fjose, A., 1998. Expression of two zebrafish homologues of the murine Six3 gene demarcates the initial eye primordia. Mech. Dev. 73, 45–57.

Sharma, K., Sheng, H.S., Lettieri, K., Li, H., Karavanov, A., Potter, S., Westphal, H., Pfaff, S.L., 1998. LIM Homeodomain factors Lhx3 and Lhx4 assign subtype identities for motor neurons. Cell 95, 817–828.

Shawlot, W., Behringer, R.R., 1995. Requirement for Lim1 in head-organizer function. Nature 374, 425–430.

Thor, S., Thomas, J.B., 1997. The Drosophila islet gene governs axon pathfinding and neurotransmitter identity. Neuron 18, 397–409.

Thor, S., Andersson, S.G.E., Tomlinson, A., Thomas, J.B., 1999. A LIM-homeodomain combinatorial code for motor-neuron pathway selection. Nature 397, 76–80.

Torigoi, E., Bennani-Baiti, I.M., Rosen, C., Gonzalez, K., Morcillo, P., Ptashne, M., Dorsett, D., 2000. Chip interacts with diverse homeodomain proteins and potentiates bicoid activity in vivo. Proc. Natl. Acad. Sci. USA 97, 2686–2691.

Toyama, R., Kobayashi, M., Tomita, T., Dawid, I.B., 1998. Expression of LIM-domain binding protein (ldb) genes during zebrafish embryogenesis. Mech. Dev. 71, 197–200.

van Meyel, D.J., O'Keefe, D.D., Jurata, L.W., Thor, S., Gill, G.N., Thomas, J.B., 1999. Chip and Apterous physically interact to form a functional complex during Drosophila development. Mol. Cell 4, 259–265.

van Meyel, D.J., O'Keefe, D.D., Thor, S., Jurata, L.W., Gill, G.N., Thomas, J.B., 2000. Chip is an essential cofactor for Apterous in the regulation of axon guidance in Drosophila. Development 127, 1823–1831.

Weihe, U., Milan, M., Cohen, S.M., 2001. Regulation of Apterous activity in Drosophila wing development. Development 128, 4615–4622.

Westerfield, M., 1989. The Zebrafish Book: A Guide for the Laboratory Use of Zebrafish (*Brachydanio rerio*), University of Oregon Press, Eugene, OR.

Windle, J.J., Weiner, R.I., Mellon, P.L., 1990. Cell lines of the pituitary gonadotrope lineage derived by targeted oncogenesis in transgenic mice. Mol. Endocrinol. 4, 597–603.